DEEP CIRCULATION IN RED GIANT STARS: A SOLUTION TO THE CARBON AND OXYGEN ISOTOPE PUZZLES?

G. J. Wasserburg[1], Arnold I. Boothroyd[2], and I.-Juliana Sackmann[3]

[1]Lunatic Asylum, Charles Arms Laboratory 170-25,
California Institute of Technology, Pasadena, CA 91125

[2]Canadian Institute for Theoretical Astrophysics, University of Toronto,
60 St. George Street, Toronto, Ontario, Canada M5S 1A7

[3]W. K. Kellogg Radiation Laboratory 106-38,
California Institute of Technology, Pasadena, CA 91125

Accepted April 1995

Appeared 1995, *Astrophysical Journal (Letters)*, **447**, L71

ABSTRACT

The long-standing puzzle of low $^{12}C/^{13}C$ in low-mass red giant branch (RGB) stars, and the more recent puzzle of low $^{18}O/^{16}O$ ratios in asymptotic giant branch (AGB) stars and in circumstellar Al_2O_3 grains preserved in meteorites, can be resolved by deep circulation currents below the bottom of the standard convective envelope. This transports matter from the non-burning bottom of the convective envelope down to regions where some CNO processing can take place ("*cool bottom processing*"). Modelling circulation with separate downward and upward streams, we found that, to resolve both discrepancies, the base of the extra mixing had to reach a temperature T_P close to that of the H-burning shell, namely, $\Delta \log T \approx 0.17$ from the base of the H-shell for both RGB and AGB. While the envelope composition depends sensitively on T_P, it is insensitive to the speed or geometry of mixing. This indicates that our stream circulation model is generic, so that more sophisticated mixing models with the same T_P would yield similar results. On the AGB, our models predict that stars with low $^{18}O/^{16}O$ can be either S or C stars, but must have low $^{12}C/^{13}C$ (~ 4) and elevated ^{14}N. Cool bottom processing also destroys ^3He, so that galactic (D+^{3}He) *decreases* with time; this removes the strongest lower limit on the baryon density Ω_b from Big Bang nucleosynthesis models.

Subject Headings: Galaxy: abundances — nuclear reactions, nucleosynthesis, abundances — stars: abundances — stars: giants — cosmology: early universe

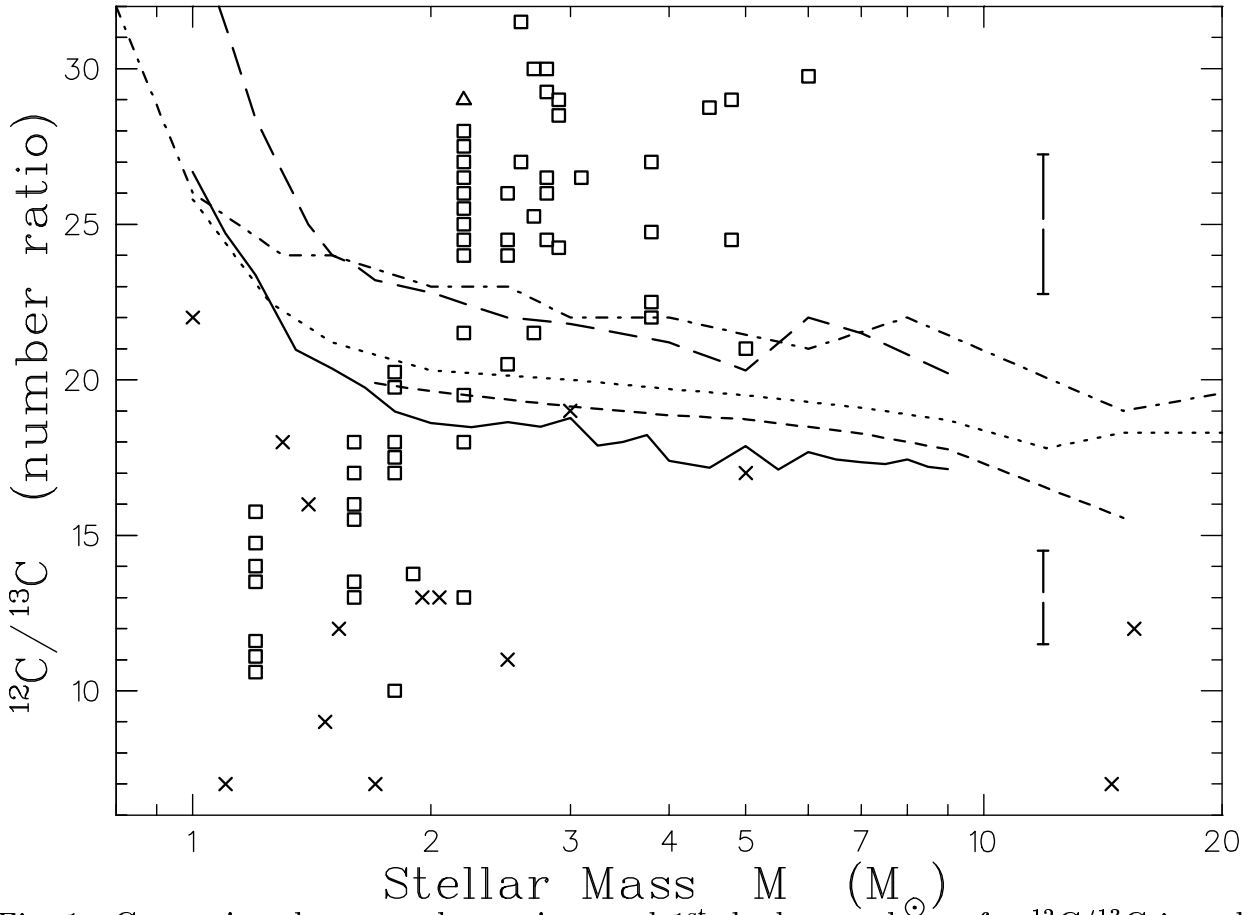

Fig. 1. Comparison between observations and 1st dredge-up theory for $^{12}C/^{13}C$ in red giants as a function of stellar mass M. Isolated stars (×) of Harris & Lambert (1984*a,b*) and Harris, Lambert, & Smith (1988) have much less accurate stellar masses than open cluster data (□) and lower limits (△) of Gilroy (1989); typical $^{12}C/^{13}C$ uncertainties are shown by error bars at right. Theory: solid line: Boothroyd & Sackmann (1995), short dashed: El Eid (1994), long dashed: Bressan et al. (1993), dotted: Schaller et al. (1992), dot-dashed: Dearborn (1992).

1. INTRODUCTION

It is known that $^{12}C/^{13}C$ in low mass red giants cannot be accounted for by standard stellar evolution theory (cf. Dearborn, Eggleton, & Schramm 1976; Gilroy 1989). In "1st dredge-up", the ^{13}C-rich pocket from main sequence burning is brought to the surface by the star's deep convective envelope; for low mass stars, this occurs near the base of the red giant branch (RGB). While theoretical predictions of $^{12}C/^{13}C$ agree with observations within $\sim$ 25% for stellar masses $\gtrsim$ 2 $M_\odot$, the predicted trend between 1 and 2 $M_\odot$ is incorrect; for 1 $M_\odot$ stars, observed $^{12}C/^{13}C$ ratios are a factor of $\sim$ 3 below calculated values (Fig. 1). A wealth of papers have interpreted this as implying some form of extra mixing to bring up more ^{13}C (recently, see e.g., Charbonnel 1994; Wallerstein & Morell 1994; and references therein); observations (Gilroy & Brown 1991) show that this must take place *subsequent* to 1st dredge-up, since low $^{12}C/^{13}C$ values do not appear until then.

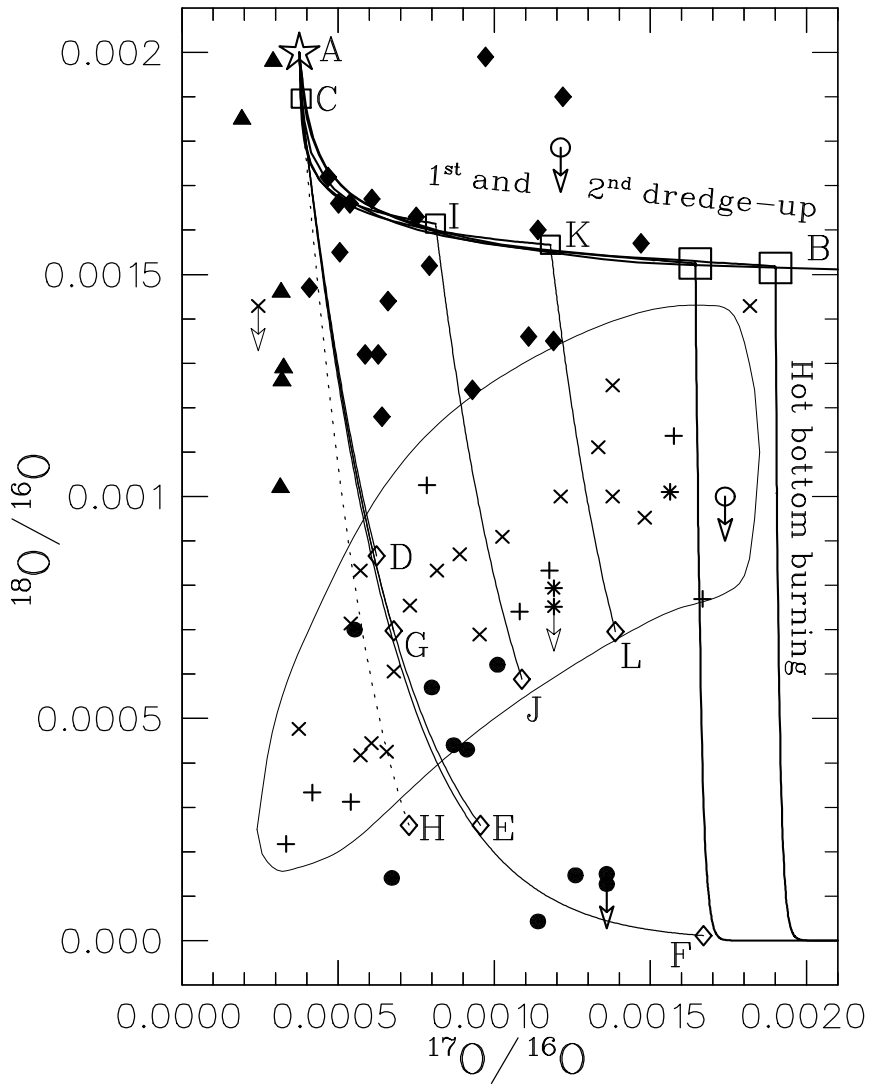

Fig. 2. Comparison of predicted $^{18}O/^{16}O$ and $^{17}O/^{16}O$ with grain and stellar observations. Two J-type carbon stars ($\circ$), with $^{12}C/^{13}C \sim 3$ indicating hot bottom burning, have only upper limits for ^{18}O. Normal S stars ($+$) and C stars ($\times$) on the AGB have large errors $\sim 50\%$ (not shown); circumstellar C star observations ($*$) of Kahane et al. (1992) are somewhat more accurate. The loop shows where most C and S star observations lie. High precision grain measurements (filled symbols: uncertainties $\sim 10\%$) are grouped as by Nittler et al. (1994): group 1 ($\blacklozenge$) are consistent with 1st and 2nd dredge-up (given some metallicity variation, which shifts point A: see BSW-I and II), group 2 ($\bullet$) display very low $^{18}O/^{16}O$ (requiring ^{18}O destruction), and group 3 ($\blacktriangle$) display low $^{17}O/^{16}O$. Initial isotope ratios are the large star at A; 1st and 2nd dredge-up shift compositions along AB. For 6 and 7 $M_\odot$, termination of 1st and 2nd dredge-up ($\square$) is followed by AGB hot bottom burning (vertical lines: region to their left, where many observations lie, cannot be populated via standard dredge-up and hot bottom burning). "Cool bottom processing" (which can populate this region) is shown by curves slanting down and to the right from termination of 1st dredge-up for 1, 1.5, and 1.65 $M_\odot$ ($\square$ at C, I, and K, respectively). For 1 $M_\odot$: CD: $\log T_P = 7.49$, CE: $\log T_P = 7.51$, CF: $\log T_P = 7.53$, all with $M_E = 0.2\,M_\odot$; CG: same as CE, but with $M_E = 0.4\,M_\odot$; dotted curve CH: same as CE, but with highest allowed ^{17}O-destruction rate. Curve IJ: 1.5 $M_\odot$ with $M_E = 0.4\,M_\odot$, KL: 1.65 $M_\odot$ with $M_E = 0.5\,M_\odot$, both with $\log T_P = 7.51$. Endpoints ($\diamond$) are for $\tau^*_{\rm AGB} = 10^6$ yr.

For $^{17}O/^{16}O$ and $^{18}O/^{16}O$, 1st and 2nd dredge-up theory is not in conflict with observations (Dearborn, Tinsley, & Schramm 1978; Landré et al. 1990; Dearborn 1992; Schaller et al. 1992; Bressan et al. 1993; El Eid 1994; Boothroyd, Sackmann, & Wasserburg 1994, hereafter BSW-I). However, a discrepancy does exist in the later asymptotic giant branch (AGB) phase. It has been shown that there is an "*inaccessible*" region in the $^{17}O/^{16}O$ vs. $^{18}O/^{16}O$ diagram (see Fig. 2), which cannot be populated by standard dredge-up or hot bottom burning (Boothroyd, Sackmann, & Wasserburg 1995: hereafter BSW-II). However, observations of AGB stars lie in this region (Harris, Lambert, & Smith 1985; Harris et al. 1987; Kahane et al. 1992). The problem is intensified by precise O-isotope data of circumstellar Al_2O_3 grains, preserved in meteorites, that are believed to come from AGB stars (Huss et al. 1992; Huss et al. 1994; Nittler et al. 1994; Nittler, private communication); some data lie in the "inaccessible" region (see Fig. 2). BSW-II pointed out that this puzzle might also be solved by some form of extra mixing ("*cool bottom processing*"), where the bottom of the convective envelope remains cool while an *ad hoc* mixing mechanism brings material down to layers hot enough for some nuclear processing. The data require that this take place in stars of 1 to 2 $M_\odot$. There is a large literature on possible mixing mechanisms, particularly for C and Li (see, e.g., Dearborn et al. 1976; Genova & Schatzmann 1979; Press & Rybicki 1981; Pinsonneault et al. 1989; Zahn 1992).

2. METHODS AND RESULTS

Parametric computations were performed, with envelope structures obtained from models of a 1 $M_\odot$ star (Sackmann, Boothroyd, & Kraemer 1993), not long after 1st dredge-up on the RGB, and prior to the first He-shell flash (thermal pulse) on the AGB. Table 1 shows the initial stellar mass M_i, luminosity L, degenerate core mass M_c, rate $\dot{M}_c$ at which the H-shell burns outward in mass, temperature log $T_{\rm H}$ at the base of the H-shell, and time $\tau^* = \tau^*_{\rm RGB}$ or $\tau^*_{\rm AGB}$ spent on the RGB or AGB, respectively. Initial RGB and AGB envelope compositions were obtained from full stellar evolutionary calculations of Boothroyd & Sackmann (1995). Nuclear rates of Caughlan & Fowler (1988) were used, except for $^{17}O + p$, where those of Landré et al. (1990) were used.

TABLE 1

	M_i ($M_\odot$)	log L	M_c ($M_\odot$)	$\dot{M}_c$ ($M_\odot$/yr)	log $T_{\rm H}$	τ^* (yr)	M_E ($M_\odot$)	log T_P	$\dot{M}_P$ ($M_\odot$/yr)	f_u/f_d
RGB:	1.0	1.6	0.251	$6 \cdot 10^{-10}$	7.473	$5 \cdot 10^7$	0.7	7.24 – 7.36	$10^{-9} - 10^{-4}$	1, 9, 99
AGB:	1.0	3.2	0.536	$3 \cdot 10^{-8}$	7.679	10^6	0.2, 0.4	7.44 – 7.60	$10^{-7} - 10^{-4}$	1, 9, 99
	1.5						0.4, 0.8	7.51, 7.53	$10^{-5}, 10^{-4}$	1
	1.65						0.5, 1.0	7.51, 7.53	$10^{-5}, 10^{-4}$	1

In our two-stream "conveyor-belt" circulation model, matter from the bottom of envelope convection streamed downward, reaching a maximum temperature T_P, then returned upward and was mixed with the convective envelope (i.e., a composition advection equation with nuclear burning, and no mixing between downward and upward streams). Envelope and stream compositions were followed through time. The value of T_P was treated as a free parameter (see Table 1); values selected for discussion were those satisfying the observational data. The other key free parameter was the stream mass flow rate $\dot{M}_P$. This must be slower than that of RGB or AGB convective envelopes ($\dot{M}_P \ll \dot{M}_{\rm conv} \sim 1\ M_\odot$/yr), while the streams must move faster than the speed with which the H-shell burns its way outward ($\dot{M}_P \gtrsim \dot{M}_c$: see Table 1). We explored a wide range of $\dot{M}_P$ values (see Table 1). We also explored the effect of varying the envelope mass M_E on the AGB, where M_E is uncertain due to the stellar wind mass loss rate.

For equal downward and upward velocities, the fractional areas at the base of the convective envelope occupied by downward and upward streams are equal. The downward stream then spends a time $\Delta t_d = 0.5\,\Delta M_r/\dot{M}_P$ in a layer ΔM_r, the upward stream spending the same time Δt_u there on its way out. When downward and upward velocities, and respective fractional areas f_d and f_u, are *not* equal, these times become $\Delta t_d = f_d \Delta M_r/\dot{M}_P$ and $\Delta t_u = f_u \Delta M_r/\dot{M}_P$. The total time spent in any mass layer is independent of f_d and f_u, for $f_d + f_u = 1$; note that $f_d + f_u < 1$ is not a separate case, being equivalent to increasing $\dot{M}_P$ while reducing the timescale τ^*. Besides $f_d = f_u = 0.5$, we considered $f_u/f_d = 9$ and $f_u/f_d = 99$. Even such large variations in f_u/f_d made essentially no difference to the resulting envelope abundances, except for ^{7}Li.

Slow deep mixing tends to be opposed by a gradient in the mean molecular weight μ. A μ-discontinuity is left behind by 1$^{\rm st}$ dredge-up; only after the H-burning shell reaches and destroys this "barrier" can circulation reach the higher-temperature domains (see, e.g., Charbonnel 1994). We infer that our reported T_P values are determined by the μ-gradient in the outer wing of the H-shell that inhibits mixing. For stellar masses above $\sim 2.3\,M_\odot$, the RGB ends before the H-shell reaches the μ-discontinuity — no RGB cool bottom processing should take place in such stars. On the early AGB, not too much cool bottom processing is expected, as the H-shell largely stops burning; one *does* expect cool bottom processing later on the AGB, when the H-shell burns strongly again (intermittently interrupted by He-shell flashes).

The calculated envelope composition depended sensitively on T_P. In the relevant RGB regime of partial CNO-processing, a change of $\Delta \log T_P = 0.03$ resulted in a factor of 2 change in ^{12}C/^{13}C. Consistency between theory and observations was achieved for $\log T_P \approx 7.30$. For $\dot{M}_P \gtrsim 10^{-8}\ M_\odot$/yr, ^{13}C/^{12}C and ^{12}C were essentially independent of $\dot{M}_P$ (and of f_u/f_d) for our RGB model. Results of our mass transport scheme are thus resilient to details of the motion except for T_P and a minimum mass transfer rate. Full dynamical models for deep mixing should thus yield results similar to the two-stream

model for similar T_P. The $\dot{M}_P$-independence is due to the low extent of nuclear processing on each circulation pass for these speeds of transport. An isotope of abundance X that burns at a rate $R_{X,r}$ will be reduced by $\Delta X_{r,d} = -XR_{X,r}\Delta t_d$ as it moves down through a layer ΔM_r (and similarly by $\Delta X_{r,u}$ on the way back up). If the total change ΔX per pass is small, then $\Delta X = \sum_r \left[\Delta X_{r,d} + \Delta X_{r,u}\right] \approx -\left(X/\dot{M}_P\right) \sum_r \left[(f_d + f_u)R_{X,r}\Delta M_r\right] \equiv -X\lambda_X/\dot{M}_P$, where λ_X is independent of $\dot{M}_P$, being the burning rate integrated over mass (not time!) through the path. If X is also produced by burning isotope Y, one obtains $\Delta X = \left(Y\lambda_Y - X\lambda_X\right)/\dot{M}_P$. Matter is delivered to the envelope at a rate $\dot{M}_P$, where it is diluted by the envelope mass M_E. Thus, in the envelope, $dX_E/dt = \left(\dot{M}_P/M_E\right)\Delta X = \left(Y\lambda_Y - X\lambda_X\right)/M_E$, independent of $\dot{M}_P$. This implies $d^{12}\mathrm{C}_E/dt = -\lambda_{12}{}^{12}\mathrm{C}_E/M_E$ and $d^{13}\mathrm{C}_E/dt = \left(\lambda_{12}{}^{12}\mathrm{C}_E - \lambda_{13}{}^{13}\mathrm{C}_E\right)/M_E$, in the approximation of small burning per pass. Solving for envelope ^{12}C and ^{13}C abundances yields

$$^{12}\mathrm{C}_E(t) = {}^{12}\mathrm{C}_E(0)\, e^{-\lambda_{12}t/M_E}\ , \tag{1}$$

$$\frac{^{13}\mathrm{C}_E(t)}{^{12}\mathrm{C}_E(t)} = \frac{^{13}\mathrm{C}_E(0)}{^{12}\mathrm{C}_E(0)}\, e^{-(\lambda_{13}-\lambda_{12})t/M_E} + \frac{\lambda_{12}}{\lambda_{13}-\lambda_{12}}\left(1 - e^{-(\lambda_{13}-\lambda_{12})t/M_E}\right)\ . \tag{2}$$

Equation (2) can be further simplified: ^{13}C burns ~ 3.5 times as fast as ^{12}C (almost independent of temperature), so $\lambda_{13}/\lambda_{12} \approx 3.5$, and $\lambda_{12}/(\lambda_{13} - \lambda_{12}) \approx 0.4$. For $\dot{M}_P \gg M_E/\tau^*_{\mathrm{RGB}}$, the above equations are in excellent agreement with full numerical calculations.

Figure 3 illustrates our RGB model results for $\log T_P \approx 7.30$. Envelope $^{12}\mathrm{C}/^{13}\mathrm{C}$ drops exponentially from 27 (as left by 1$^{\mathrm{st}}$ dredge-up) to ~ 5, spending much time in the range $15 \gtrsim {}^{12}\mathrm{C}/^{13}\mathrm{C} \gtrsim 7$ where most observations for $\sim 1\, M_\odot$ stars lie (see Fig. 1). From 1 to $\sim 2.3\, M_\odot$, increasing the stellar mass implies larger M_E and shorter τ^*_{RGB}, and thus higher $^{12}\mathrm{C}/^{13}\mathrm{C}$, in agreement with the observed trend (recall that no cool bottom processing is expected above $\sim 2.3\, M_\odot$). We conclude that excellent agreement is obtained between the observations and this cool bottom processing model, in which $\log T_P$ differs by $\Delta \log T \approx 0.17$ from the H-shell temperature $\log T_{\mathrm{H}}$ (see Table 1). Note that ^{12}C and ^{14}N abundances change by only $\sim 20\%$, while O-isotopes are essentially unaffected. The ^{9}Be abundance is decreased; ^{7}Li may either decrease, or increase via the Cameron-Fowler mechanism, depending on $\dot{M}_P$ and f_u/f_d (a future paper will discuss this).

Big bang nucleosynthesis models convert an upper bound on primordial $(\mathrm{D} + {}^3\mathrm{He})/\mathrm{H}$ into a lower bound on the baryon density Ω_b. To infer primordial $(\mathrm{D} + {}^3\mathrm{He})/\mathrm{H}$, one must consider galactic chemical evolution. Deuterium is burned to ^{3}He during protostellar collapse, but this does not affect the sum $(\mathrm{D} + {}^3\mathrm{He})$ on the main sequence. However, 1$^{\mathrm{st}}$ dredge-up substantially enhances ^{3}He, by a factor of ~ 6 for $1\, M_\odot$, and by ~ 2 for $2\, M_\odot$; only above $\sim 4\, M_\odot$ is ^{3}He depleted (Iben 1967; Boothroyd & Sackmann 1995). As low mass stars are more common, stellar processing would increase galactic $(\mathrm{D} + {}^3\mathrm{He})/\mathrm{H}$; the presolar value has thus been used as an upper limit to the primordial value. Hogan (1995)

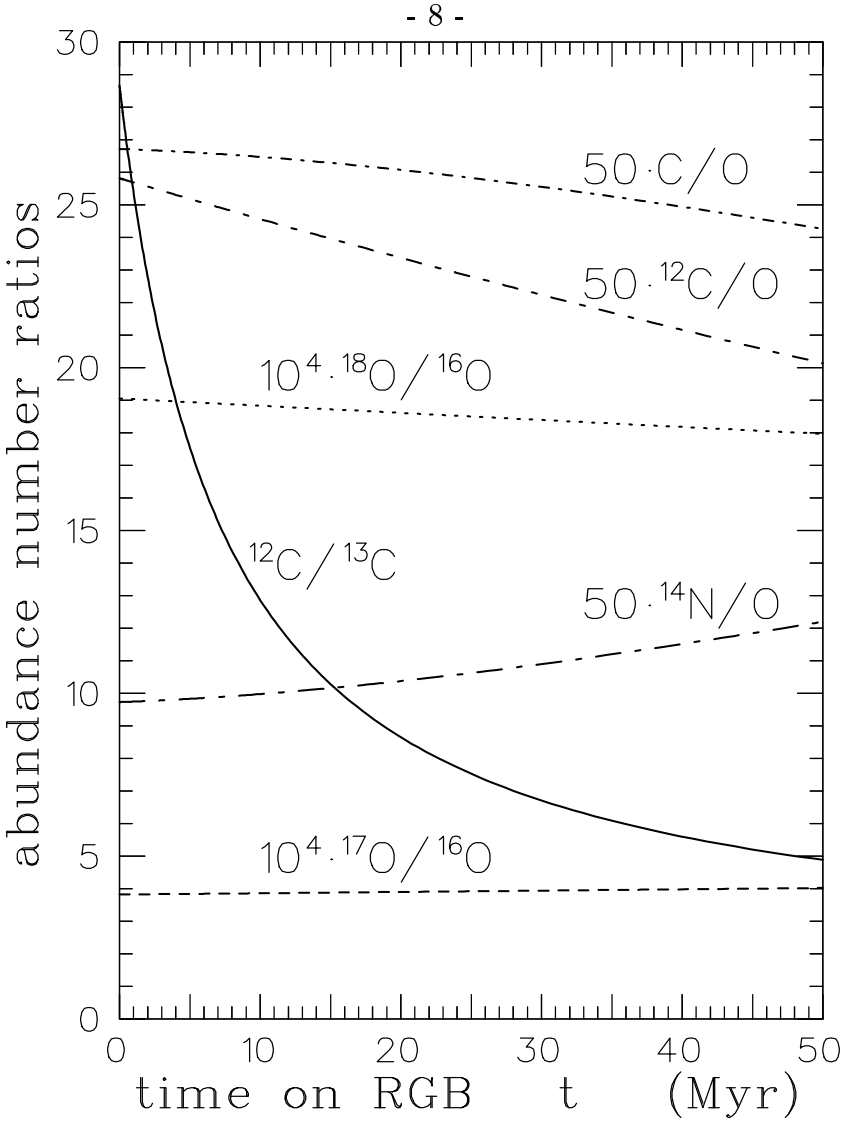

Fig. 3. Envelope composition as a function of time on the RGB for a 1 $M_\odot$ star with envelope mass $M_E = 0.7\,M_\odot$, for mixing reaching a temperature $\log T_P = 7.30$ with mass flow rate $\dot{M}_P = 10^{-4}\,M_\odot/\mathrm{yr}$, and $f_d = f_u = 0.5$.

pointed out that CNO processing sufficient to explain the $^{12}C/^{13}C$ observations in low mass stars should also destroy ^{3}He, perhaps resulting in net reduction of (D + ^{3}He)/H. Our models confirm this. For a 1 $M_\odot$ star, after 1$^{\mathrm{st}}$ dredge-up ^{3}He enhancement (by ~ 6), RGB cool bottom processing reduces ^{3}He by a factor of ~ 10, yielding net depletion by a factor of ~ 2. Both enhancement and reduction are less for higher stellar masses, but probably still result in (D + ^{3}He) depletion for stars of $\lesssim 2\,M_\odot$. Hence, stellar processing should *reduce* galactic (D + ^{3}He)/H. The primordial value must thus be larger than the present estimate, removing the strongest lower bound on the baryon density.

For the AGB, envelope compositions were also nearly independent of $\dot{M}_P$ and f_d/f_u, but depended sensitively on T_P (see points D, E, and F in Fig. 2). A temperature of $\log T_P \approx 7.51$ was able to populate the hitherto inaccessible region of the $^{18}O/^{16}O$ vs. $^{17}O/^{16}O$ diagram (curves CE, IJ, and KL in Fig. 2), achieving excellent agreement with

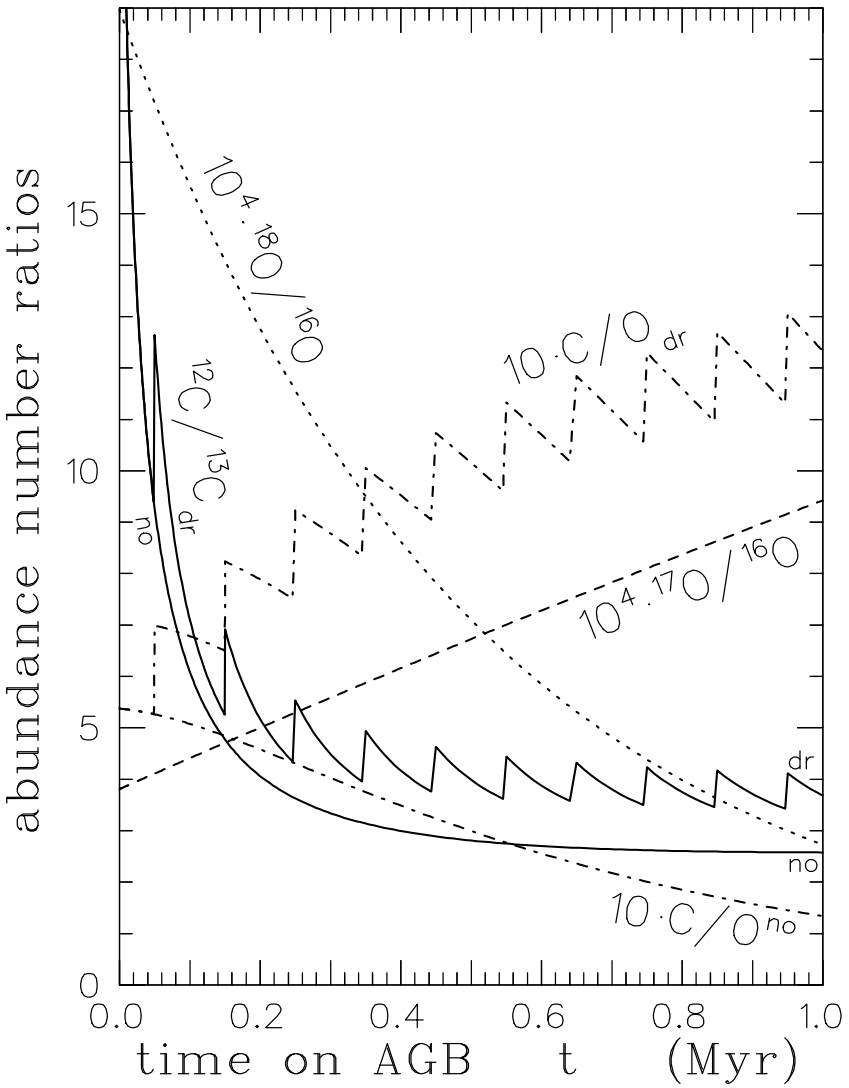

Fig. 4. Envelope composition as a function of time on the AGB for a 1 $M_\odot$ star with $M_E = 0.2\,M_\odot$, $\log T_P = 7.51$, $\dot{M}_P = 10^{-4}\,M_\odot$/yr, and $f_d = f_u = 0.5$. (Note that starting from the final RGB cool bottom processing composition, rather than the 1st dredge-up composition, would be equivalent to chopping off the left-hand 10% of the graph.) Note the regular decrease in $^{18}O/^{16}O$ and increase in $^{17}O/^{16}O$; these are unaffected by 3rd dredge-up. The curves labelled "no" correspond to evolution without 3rd dredge-up, and show a decrease in C/O and $^{12}C/^{13}C$. Sawtooth curves labelled "dr" include periodic 3rd dredge-up, which yields increasing C/O while leaving low $^{12}C/^{13}C$.

observed O-isotope ratios. Note that this T_P differs by the same amount $\Delta \log T = 0.17$ from the AGB H-shell temperature as on the RGB, as expected from the μ-gradient argument. Figure 4 shows the results: $^{18}O/^{16}O$ drops by a factor of ~ 7, and $^{17}O/^{16}O$ grows by a factor of ~ 2.5 (cf. curve CE of Fig. 2). The ^{18}O abundance decays exponentially with time on the AGB (like ^{12}C on the RGB). The behavior of ^{17}O is governed by an equation similar to that of ^{13}C on the RGB.

The effect of AGB cool bottom processing on C-isotopes is of key interest. This is complicated by periodic He-shell flashes, which can dredge up significant amounts of ^{12}C

("3rd dredge-up") and may produce a carbon star. For a 1 $M_\odot$ star, the core mass increases by $\sim 0.003\,M_\odot$ due to H-shell burning in each $\sim 10^5$ yr period between flashes (Sackmann et al. 1993). Typically, one might expect $\sim 1/3$ of this (of which 25% by mass is ^{12}C) to be dredged up in each flash. Such dredge-up was added parametrically to our models, as shown by the sawtoothed curves of C/O (dr) and ^{12}C/^{13}C (dr) of Figure 4; the smooth curves (no) are for no 3rd dredge-up. Reasonable amounts of 3rd dredge-up may still yield a carbon star, despite ^{12}C destruction; the case of Figure 4 is an S star for the first half of its AGB lifetime, and a C star for the second half. However, when cool bottom processing occurs, obtaining C/O > 1 may require more carbon dredge-up per flash than is generally assumed (cf. Busso et al. 1993), making it more difficult to produce carbon stars of $\sim 1\,M_\odot$. In addition, AGB cool bottom processing results in ^{12}C/^{13}C ~ 4, even when 3rd dredge-up is present. This large envelope ^{13}C does *not* help with the puzzle of the *s*-process ^{13}C neutron source, as the H-shell burns ^{13}C to ^{14}N. Indeed, it poses a new puzzle, namely, how to account for AGB stars with low ^{18}O/^{16}O but high ^{12}C/^{13}C. Note that cool bottom processing also results in large ^{14}N enrichments, by a factor of 3 to 6.

Full stellar evolutionary models that include some dynamical prescription for extra mixing are needed to investigate the interaction between cool bottom processing, 3rd dredge-up, and C star formation. However, such models should yield results similar to our parametric models, if the mixing reaches a similar temperature T_P; the increase in T_P as stars climb the RGB or AGB should be largely offset by the faster timescales τ^*, since different CNO-burning rates have a similar temperature dependences.

This paper was much improved by penetrating comments and creative suggestions by M. Busso, and critical reading and comments by G. Huss, G. Bazan, C. A. Barnes, R. F. Christy, and R. Gallino. One of us (A. I. B.) wishes to thank S. D. Tremaine and P. G. Martin for the support provided by the Canadian Institute for Theoretical Astrophysics. This work was supported in part by a grant from the Natural Sciences and Engineering Research Council of Canada, NASA grants NAGW-3040, NAGW-3337, and NAGW-3297. [This paper is Contribution No. 5498(892) of the Division of Geological and Planetary Sciences of the Caltech.]

REFERENCES

Boothroyd, A. I., & Sackmann, I.-J. 1995, in preparation

Boothroyd, A. I., Sackmann, I.-J., & Wasserburg, G. J. 1994, ApJ, 430, L77 (BSW-I)

———. 1995, ApJ, 442, L21 (BSW-II)

Bressan, A., Fagotto, F., Bertelli, G., & Chiosi, C. 1993, A&AS, 100, 647

Busso, M., Chieffi, A., Gallino, R., Limougi, M., Raiteri, C. M., & Straniero, O. 1993, in ZAU Symposium 153: Planetary Nebulae, ed. R. Weinberg & A. Acker (Dordrecht: Kluwer), 361

Caughlan, G. R., & Fowler, W. A. 1988, Atomic Data Nucl. Data Tables, 40, 205
Charbonnel, C. 1994, A&A, 282, 811
Dearborn, D. S. P. 1992, Phys. Reports, 210, 367
Dearborn, D., Tinsley, B. M., & Schramm, D. N. 1978, ApJ, 223, 557
Dearborn, D., Eggleton, P. P., & Schramm, D. N. 1976, ApJ, 203, 455
El Eid, M. F. 1994, A&A, 285, 915
Genova, F., & Schatzmann, E. 1979, A&A, 78, 323
Gilroy, K. K. 1989, ApJ, 347, 835
Gilroy, K. K., & Brown, J. A. 1991, ApJ, 371, 578
Harris, M. J., & Lambert, D. L. 1984*a*, ApJ, 281, 739
———. 1984*b*, ApJ, 285, 674
Harris, M. J., Lambert, D. L., Hinkle, K. H., Gustafsson, B., & Eriksson, K. 1987, ApJ, 316, 294
Harris, M. J., Lambert, D. L., & Smith, V. V. 1985, ApJ, 299, 375
———. 1988, ApJ, 325, 768
Hogan, C. J. 1995, ApJ, 441, L17
Huss, G. R., Fahey, A. J., Gallino, R., & Wasserburg, G. J., 1994, ApJ, 430, L81
Huss, G. R., Hutcheon, I. D., Wasserburg, G. J., & Stone, J. 1992, Lunar Planet. Sci., 23, 563
Iben, I., Jr. 1967, ApJ, 147, 624
Kahane, C, Cernicharo, J., Gómez-González, J., & Guélin, M. 1992, A&A, 256, 235
Landré, V., Prantzos, N., Aguer, P., Bogaert, G., Lefebvre, A., & Thibaud, J. P. 1990, A&A, 240, 85
Nittler, L. R., Alexander, C. M. O'D., Gao, X., Walker, R. M., & Zinner, E. K. 1994, Nature, 370, 443
Pinsonneault, M. H., Kawaler, S. D., Sofia, S., & Demarque, P. 1989, ApJ, 338, 424
Press, W. H., & Rybicki, G. B. 1981, ApJ, 248, 751
Sackmann, I.-J., Boothroyd, A. I., & Kraemer, K. E. 1993, ApJ, 418, 457
Schaller, G., Schaerer, D., Meynet, G., & Maeder, A. 1992, A&AS, 96, 269
Wallerstein, G., & Morell, O. 1994, A&A, 281, L37
Zahn, J. P. 1992, A&A, 265, 115